ARTICLE

Direct Low-Temperature Nanographene CVD Synthesis over a Dielectric Insulator

Mark H. Rümmeli,[†,‡,*] Alicja Bachmatiuk,[†] Andrew Scott,[†,§] Felix Börrnert,[†] Jamie H. Warner,[⊥] Volker Hoffman,[†] Jarrn-Horng Lin,[∥] Gianaurelio Cuniberti,[§] and Bernd Büchner[†]

[†]IFW Dresden, P.O. Box 270116, 01171 Dresden, Germany, [‡]Department of Physics, Technische Universität Dresden, 01062 Dresden, Germany, [§]Institute for Materials Science and Max Bergmann Center of Biomaterials, Dresden University of Technology, 01062 Dresden, Germany, [⊥]Department of Materials, University of Oxford, Parks Road, Oxford OX1 3PH, United Kingdom, and [∥]Department of Material Science, National University of Tainan, 33, Sec. 2, Shu-Lin Street, Tainan, Taiwan 700, Republic of China

ABSTRACT Graphene ranks highly as a possible material for future high-speed and flexible electronics. Current fabrication routes, which rely on metal substrates, require post-synthesis transfer of the graphene onto a Si wafer, or in the case of epitaxial growth on SiC, temperatures above 1000 °C are required. Both the handling difficulty and high temperatures are not best suited to present day silicon technology. We report a facile chemical vapor deposition approach in which nanographene and few-layer nanographene are directly formed over magnesium oxide and can be achieved at temperatures as low as 325 °C.

KEYWORDS: graphene · chemical vapor deposition · transmission electron microscopy · synthesis · catalysis

Graphene is a remarkable material with incredible electrical and mechanical properties. However, it has only recently been isolated.[1] This has made graphene the "new rising star" in nanocarbon-based materials due to its exciting properties at the nanoscale, such as high charge carrier mobility.[2] In addition, when formed into narrow strips or ribbons (*ca.* 10 nm wide), a band gap opens, making them excellent candidates for field-effect transistors.[3] Hence, apart from the exciting possibilities in discovering new chemistry and physics from these 2D structures, they offer tantalizing opportunities for the development of high-speed (and even flexible) molecular electronics. However, one of the major barriers impeding their progress on this front relates to difficulties in their fabrication. In order for graphene to make significant improvements to present day technologies, it needs to be synthesized in a manner suitable for planar fabrication technologies where reproducibility is essential. Randomly placed and structured graphene flakes are not suitable for this. Epitaxial grown graphene from SiC wafers seems to be a promising route for large area growth.[4] Chemical vapor deposition (CVD) grown graphene on metals has the drawback that the graphene needs to be transferred onto a wafer after synthesis.[5] Routes which can deposit graphene or few-layer graphene on dielectric surfaces are much needed. A recently developed route to achieve this has been shown by Ismach *et al.*, in which they grow graphene on a sacrificial Cu layer which dewets and evaporates away during synthesis.[6] The technique is exciting but runs the risk of Cu contamination. A possible alternative route is the use of dielectric surface itself to directly form graphene layers *via* CVD. This is attractive because most of today's transistor technology uses complementary metal-oxide semiconductor (CMOS) technology in which an oxide layer insulates the transistor gate from the channel. Hence, the ability to synthesize graphene directly on an oxide crucially removes the need to transfer the graphene after synthesis and can remove the need for large-area synthesis as required with metal substrates.[7] Moreover, in order for the technique to be easily adapted for use in Si-based technology, low-temperature reactions (400−450 °C) are required to maintain the mechanical integrity of low dielectric constant (K) intermetal dielectrics.[8] We have previously shown the potential for oxides to graphitize carbon.[9,10] Recent studies using silicon oxide,[11,12] alumina,[13] and zirconia[14] to grow single-walled carbon nanotubes corroborate that oxides can graphitize carbon. In this report, we conclusively demonstrate that MgO is suitable for the direct fabrication of nanographene and few-layer nanographene (nFLG) *via* CVD. Moreover, adjusting the reaction time or temperature allows one to switch between nFLG and nanographene formation. We have achieved synthesis temperatures down to 325 °C using acetylene as the feedstock.

*Address correspondence to m.ruemmeli@ifw-dresden.de.

Received for review May 5, 2010 and accepted June 18, 2010.

Published online June 29, 2010. 10.1021/nn100971s

RESULTS AND DISCUSSION

Figure 1 presents a series of low-voltage third-order aberration-corrected HRTEM data from samples prepared *via* catalytic CVD reactions on MgO using cyclohexane as the feedstock. Figure 1A,B presents a MgO crystal after a CVD reaction in cyclohexane at 875 °C with a reaction time of 5 min. Graphitic layers (2−10) are seen on the surface of the nanocrystals and have an interspacing of *ca.* 3.5 Å. The graphitic layers align themselves with the MgO [100] lattice planes (spacing 0.21 nm), bending if necessary to do so. In other words, the graphene layers anchor to the MgO crystal. Most graphene layers anchor into every second lattice plane. However, every so often, they anchor to a consecutive plane, presumably to minimize the strain. This is similar to the manner in which graphitic layers formed through SiC decomposition anchor to SiC.[15] For reaction times between 5 min and 1 h, the number of graphene layers formed is always the same, ranging between 2 and 10 layers. By reducing the reaction time, one can tune the reaction to yield single graphene layers on the surface. Figure 1C−F shows cross-sectional views and top views of graphene nanoislands on the surface of the oxide crystals. To confirm the formation of graphene, the samples were immersed in HCl (5 M) to dissolve the MgO. After this step, the samples were thoroughly washed and then annealed in vacuum (10^{-6} mbar at 500 °C for 60 min) to remove any functional groups that may have attached during the purification procedure. IR spectroscopy confirmed that no functional groups were present after annealing in vacuum. The process leaves only nanographite or nanographene shells, as shown in Figure 1G,H.

The Raman spectra (Figure 2) from the samples show the G mode (due to bond stretching between pairs of sp^2 carbon atoms) and the D peak (due to breathing modes of sp^2 carbon atoms in rings), which lie around 1580 and 1360 cm^{-1}, respectively, and provide further confirmation for graphitic carbon formation. Usually, for graphene and few-layer graphene, one obtains an intense and narrow G band, a weak D mode and a very intense 2D mode at *ca.* 2700 cm^{-1}. The 2D mode is the second-order D mode, and its intensity is dependent on the number of layers.[16] These features are clearly not obtained from our samples, as can be seen in Figure 2A,B. Instead, we obtain a strong D mode and a broadened G mode and a weak and broad D mode. These differences occur due to the samples being composed of nanographene. The nanosized graphene domains formed in our CVD route have a large number of edge states relative to the bulk (nano) graphene structure (see Figure 2D). Ferrari discusses in detail the effects of edge states, which are essentially defects.[16] He states that the edge states give rise to a D band. In addition, the G band is broadened, and the average G position shifts up from around 1580 to 1600 cm^{-1}. Moreover, the doublet structure of the D and 2D mode is lost. These effects are exactly what we observe in our Raman spectra and are fully concomitant with nanographitic species. In addition, Cançado *et al.* have shown that one can successfully determine the crystallite size, L_a (nm), of nanographite by Raman spectroscopy using the general equation $L_a = (2.4 \times 10^{-10})\lambda_l^4(I_D/I_G)^{-1}$, where λ_l is the laser energy in nanometers, I_D and I_G are the intensity of the D and G modes, respectively.[17] From the above equation, we obtain nanographene domain sizes of around 50 nm. This is reasonable given that the MgO nanocrystals over which the nanographene and few-layer nanographene are

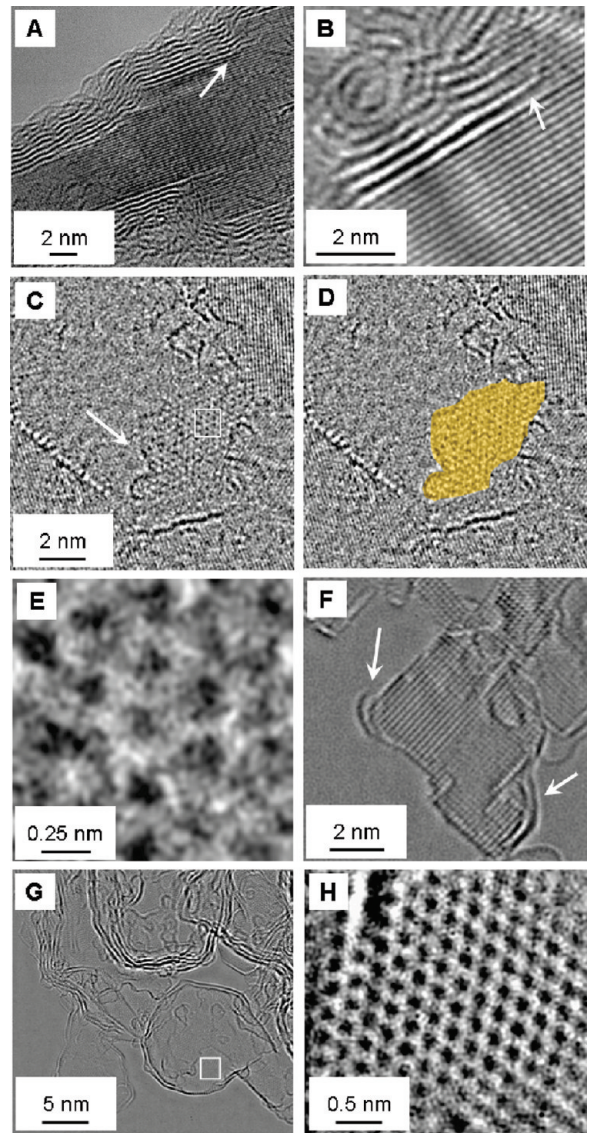

Figure 1. (A) TEM image of few-layer graphene on a MgO crystal. Note that the graphene layers interface directly to the MgO lattice fringes (A,B) [cyclohexane, 875 °C, 5 min]. (C,D) Graphene island on the surface of a MgO crystal [cyclohexane, 875 °C, 30 s]. (E) Magnified region from the box in panel C highlighting the graphene structure. (F) Cross-section view of graphene on the surface of a MgO crystal. (G) Graphene shells after removal of MgO [cyclohexane, 875 °C, 1 h]. (H) Magnified region from the box in panel C highlighting graphene structure.

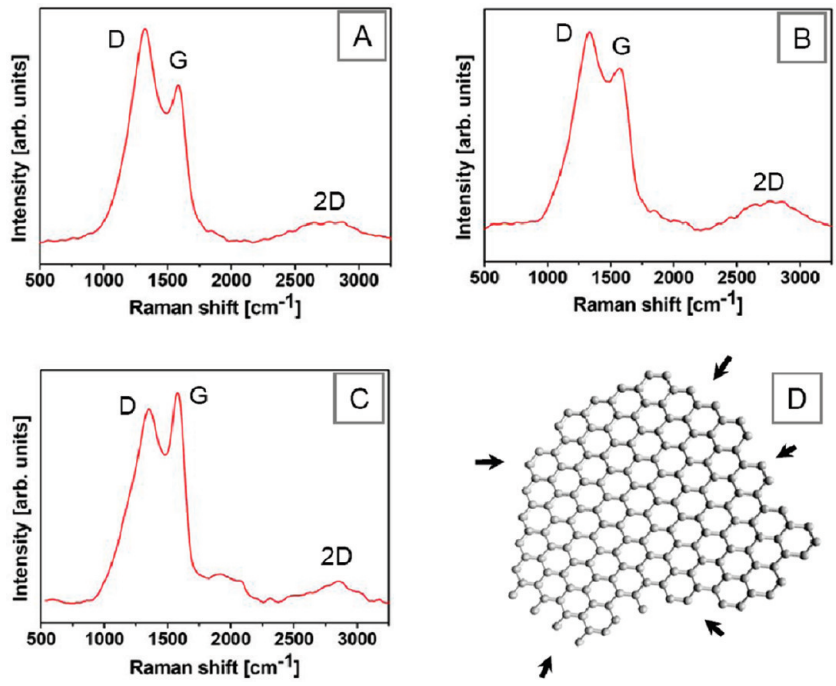

Figure 2. (A,B) Raman spectra of nanographite from a purified sample prepared at 875 °C over MgO with a cyclohexane feedstock. Reaction time for A was 30 s and B was 5 min. (C) Raman spectrum from a purified sample prepared at 325 °C over MgO with cyclohexane as the feedstock and a reaction time of 10 min. (D) Schematic of a nanographene flake illustrating the large number of edge defects relative to the bulk nanographene sheet. The high number of edge defects relative to the honeycomb structure of the bulk flake leads to a high D band in the Raman spectra.

grown vary in size from several nanometers to a few hundred nanometers.

The use of C_2H_2 for the low-temperature CVD synthesis of carbon nanotubes has previously been shown with temperatures as low as 350 °C.[18] The ability to synthesize graphene *via* CVD at low temperature is important for direct device integration. Hence, we also explored the use of acetylene for graphene formation on MgO at 370 and 325 °C. With a reaction time of 10 min, we obtained nanosized graphene islands on the surface. Some islands could be observed to align with the [100] lattice planes of the crystal. Figure 3 shows these traits for samples synthesized at 370 °C (panel A) and 325 °C (panel B). The data show the successful formation of nanographene at 325 °C. To confirm the presence of nanographene, the samples were purified for further investigation. TEM studies showed the purified samples to consist of nanographite. Figure 3C shows a typical sample in which various Moiré patterns can be observed. Fast Fourier transform data from the acquired micrographs consistently showed spot sequences and spacing arising from the [100] graphite lattice plane (*e.g.*, Figure 3D). In addition, measurements showed interlayer spacing of 3.5 Å concomitant with the interlayer spacing in graphite, as shown, for example, in panel E. The samples were also subjected to Raman spectroscopic investigations. However, no signal was obtained for the as-produced sample. This is due to the number of graphitic nanoislands being limited, making the total signal very weak. Raman spectra were obtained from the purified samples, as the sample now comprises entirely agglomerated nanographene, *viz.*, nanographite. The Raman spectra (Figure 3C) showed the presence of the G and D modes, authenticating sp^2 carbon synthesis at the low temperature of 325 °C. The mean crystallite sizes, estimated from the Raman spectra, were around 30 nm. This is larger than the estimates from TEM for the nanographene flakes which range from 2 to 5 nm. The discrepancy may be due to nanographene islands coalescing during the purification process. The coalescence of the nanographene islands reduces the number of unsaturated bonds (edge states) and hence reduces energy.

The effect of extended reaction times (up to 2 h) was also investigated. The results showed an increase in the number islands on the surface of the MgO nanocrystals. For samples formed with a 2 h reaction time, occasionally 2 or 3 graphitic layers could be observed. However, for the most part, the surface was covered with nanographene islands, as illustrated in Figure 3F,G.

CONCLUSION

The results clearly demonstrate that nanographene can be grown directly on MgO. Similar to earlier FLG studies, samples formed at higher temperatures show graphene layers anchored to crystal planes.[10,15] Moreover, with the higher reaction temperature of 875 °C, the number of layers is always limited regardless of reaction time. This hints that the incorporation of carbon atoms to the nanographene network occurs at the crystal/graphene layer interface, *viz.*, bottom-up growth. Such a growth process is fundamentally

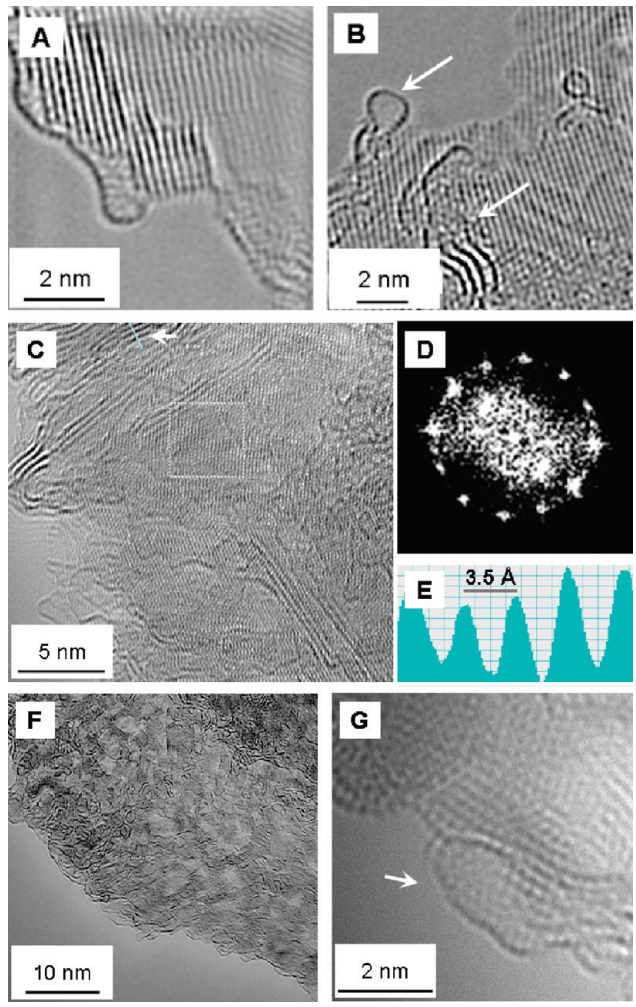

Figure 3. (A) Graphene layer at the edge of a MgO crystallite [acetylene, 370 °C, 10 min]. (B) Graphene layer interfacing with MgO lattice fringes and graphene nanoislands on the surface/edge [acetylene, 325 °C, 10 min]. Note: The images have been reconstructed using a mask applied to a 2D fast Fourier transform of the image. (C) Purified graphite from graphene formed on MgO [acetylene, 325 °C, 10 min]. (D) Fast Fourier transform image from the region (square) marked in panel D, showing the diffraction patterns from (100) graphite. (E) Contrast from interlayer graphite taken from panel C (see arrow). (F) Dense nanographene island formation on MgO after a 2 h reaction period [acetylene, 325 °C, 2 h]. (G) Nanographene island on the edge of a MgO nanocrystal [acetylene, 325 °C, 2 h].

different than the growth mechanisms argued for other graphene routes. As pointed out by Sutter,[4] the development of an atomically precise "bottom-up" synthesis of graphene nanostructures would be a true leap forward. However, the presented data do not conclusively show this. The large number of nanographene islands formed at lower temperatures with longer reaction times indicates that island coalescence *via* Smoluchowski ripening cannot be ruled out.[19]

Our results show that MgO is suitable as a support for the synthesis of nanographene *via* CVD. Moreover, the route allows nanographene to be formed at low temperatures down to 325 °C. The technique can avoid the need for post-synthesis transfer. Moreover, because it is also accessible at low temperatures, it may hold promise for the fabrication of large area as well as nanoribbon graphene using current Si-based technologies.

EXPERIMENTAL SECTION

The CVD setup consisted of a purpose-built horizontal tube furnace with a quartz tube reactor. High-purity MgO nanocrystal powder (Alfa Aesar, purity 99.99%) was placed in an alumina crucible. Prior to synthesis, the reactor was first evacuated down to 1 hPa, after which the hydrocarbon was introduced. Both static feedstock conditions (cyclohexane at 10 kPa, static flow) and flowing conditions (acetylene/argon at 100 kPa, 600 sccm) were used. Synthesis temperatures between 875 and 325 °C were explored. Reaction times between 1 h and 10 s were investigated. The as-produced samples were investigated using third-order aberration-corrected transmission electron microscopy (FEI Titan 300-80) operating at 80 kV. Raman spectroscopy was conducted with a ThermoScientific SmartRaman spectrometer. The available lasers are 780, 633, and 532 nm.

Acknowledgment. M.H.R. thanks the EU and the Free State of Saxony for support *via* ECEMP. A.B. thanks the Alexander von

Humboldt Foundation. A.S. thanks the EU for support *via* its ERASMUS program. We are grateful to S. Leger, R. Schönfelder, M. Ulbrich, and R. Hübel for technical support.

REFERENCES AND NOTES

1. Novoselov, K. S.; Geim, A. K.; Morozov, S. V.; Jiang, D.; Zhang, Y.; Dubunos, S. V.; Grigoriava, I. V.; Firsov, A. A. Electric Field Effect in Atomically Thin Carbon Films. *Science* **2004**, *306*, 666–669.
2. Novoselov, K. S.; Geim, A. K.; Morozov, S.; Jiang, D.; Katsnelson, M. I.; Grigorieva, I. V.; Dubonos, S. V.; Firsov, A. A. Two-Dimensional Gas of Massless Dirac Fermions in Graphene. *Nature* **2005**, *438*, 197–200.
3. Ponomarenko, L. A.; Schedin, F.; Katsnelson, M. I.; Yang, R.; Hill, E. W.; Novoselov, K. S.; Geim, A. K. Chaotic Dirac Billiard in Graphene Quantum Dots. *Science* **2008**, *320*, 356–358.
4. Sutter, P. Epitaxial Graphene: How Silicon Leaves the Scene. *Nat. Mater.* **2009**, *8*, 171–172.
5. Obraztsov, A. N. Chemical Vapour Deposition: Making Graphene on a Large Scale. *Nat. Nano* **2009**, *4*, 212–213.
6. Ismach, A.; Druzgalski, C.; Penwell, S.; Schwartzberg, A.; Zheng, M.; Javey, A.; Bokor, J.; Zhang, Y. Direct Chemical Vapor Deposition of Graphene on Dielectric Surfaces. *Nano Lett.* **2010**, *10*, 1542–1548.
7. Li, X. S.; Cai, W. W.; An, J. H.; Kim, S.; Nah, J.; Yang, D. X.; Piner, R. D.; Velamakanni, A.; Jung, I.; Tutuc, E.; Banerjee, S. K.; Colombo, L.; Ruoff, R. S. Large-Area Synthesis of High-Quality and Uniform Graphene Films on Copper Foils. *Science* **2009**, *324*, 1312–1314.
8. Morgen, M.; Ryan, E. T.; Zhao, J. H.; Hu, C.; Cho, T. H.; Ho, P. S. Low Dielectric Constant Materials for ULSI Interconnects. *Annu. Rev. Mater. Sci.* **2000**, *30*, 645–680.
9. Rümmeli, M. H.; Borowiak-Palen, E.; Gemming, T.; Pichler, T.; Knupfer, M.; Kalbác, M.; Dunsch, L.; Jost, O.; Silva, S. R. P.; Pompe, W.; Büchner, B. Novel Catalysts, Room Temperature, and the Importance of Oxygen for the Synthesis of Single-Walled Carbon Nanotubes. *Nano Lett.* **2005**, *5*, 1209–1215.
10. Rümmeli, M. H.; Kramberger, C.; Grüneis, A.; Ayala, P.; Gemming, T.; Büchner, B.; Pichler, T. On the Graphitization Nature of Oxides for the Formation of Carbon Nanostructures. *Chem. Mater.* **2007**, *19*, 4105–4107.
11. Liu, B.; Ren, W.; Gao, L.; Li, S.; Pei, S.; Liu, C.; Jiang, S.; Cheng, H. M. Metal-Catalyst-Free Growth of Single-Walled Carbon Nanotubes. *J. Am. Chem. Soc.* **2009**, *131*, 2082–2083.
12. Huang, S.; Cai, Q.; Chen, J.; Qian, Y.; Zhang, L. Metal-Catalyst-Free Growth of Single-Walled Carbon Nanotubes on Substrates. *J. Am. Chem. Soc.* **2009**, *131*, 2094–2095.
13. Liu, H.; Takagi, D.; Ohno, H.; Chiashi, S.; Chokan, T.; Homma, Y. Growth of Single-Walled Carbon Nanotubes from Ceramic Particles by Alcohol Chemical Vapor Deposition. *Appl. Phys. Exp.* **2008**, *1*, 014001-1–014001-3.
14. Steiner, S. A., III; Baumann, T. F.; Bayer, B. C.; Blume, R.; Worsley, M. A.; Moberly-Chan, W. J.; Shaw, E. L.; Schloegl, R.; Hart, A. J.; Hofmann, S.; Wardle, B. L. Nanoscale Zirconia as a Nonmetallic Catalyst for Graphitization of Carbon and Growth of Single- and Multiwall Carbon Nanotubes. *J. Am. Chem. Soc.* **2009**, *131*, 12144–12154.
15. Kusunoki, M.; Rokkaku, M.; Suzuki, T. Epitaxial Carbon Nanotube Film Self-Organized by Sublimation Decomposition of Silicon Carbide. *Appl. Phys. Lett.* **1997**, *71*, 2620–2622.
16. Ferrari, A. C. Raman Spectroscopy of Graphene and Graphite: Disorder, Electron−Phonon Coupling, Doping and Nonadiabatic Effects. *Solid State Commun.* **2007**, *143*, 47–57.
17. Cancado, L. G.; Takai, K.; Enoki, T.; Endo, M.; Kim, Y. A.; Mizusaki, H.; Jorio, A.; Coelho, L. N.; Magalhaes-Paniago, R.; Pimenta, M. A. General Equation for the Determination of the Crystallite Size L_a of Nanographite by Raman Spectroscopy. *Appl. Phys. Lett.* **2006**, *88*, 163106-1–163106-3.
18. Cantoro, M.; Hofmann, S.; Pisana, S.; Scardaci, V.; Parvez, A.; Ducati, C.; Ferrari, A. C; Blackburn, A. A. M.; Wang, K. Y.; Robertson, J. Catalytic Chemical Vapor Deposition of Single-Wall Carbon Nanotubes at Low Temperatures. *Nano Lett.* **2006**, *6*, 1107–1112.
19. Coraux, J.; N'Diaye, A. T.; Engler, M.; Busse, C.; Wall, D.; Buckanie, N.; Meyer zu Heringdorf, F.-J.; van Gastel, R.; Poelsema, B.; Michely, T. Growth of Graphene on Ir(111). *New J. Phys.* **2009**, *11*, 023006/1–023006/22.